J Solid State Electrochem (2011) 15:571–577
DOI 10.1007/s10008-010-1125-6

ORIGINAL PAPER

Porous cobalt hydroxide film electrodeposited on nickel foam with excellent electrochemical capacitive behavior

Ling-Bin Kong · Mao-Cheng Liu · Jun-Wei Lang · Min Liu · Yong-Chun Luo · Long Kang

Received: 7 April 2010 / Revised: 1 June 2010 / Accepted: 9 June 2010 / Published online: 24 June 2010

Abstract A new porous cobalt hydroxide film has been successfully electrodeposited on nickel foam from 0.1 M cobalt nitrate electrolyte at −1.0 V vs. SCE without adding any surfactant. The microstructure and surface morphology of prepared cobalt hydroxide films were physically characterized by X-ray diffraction analysis and scanning electron microscopy. The results indicate that an interlaced network structure was obtained. The effects of electrodeposition time, deposition potential, and different substrates on the specific capacitance and microstructure of prepared porous α-$Co(OH)_2$ thin film were systematically studied. The results indicate that the film deposited on nickel foam at −1.0 V has excellent electrochemical properties. A maximum specific capacitance of 1473 F g^{-1} could be achieved at a current density of 2 A g^{-1}.

Keywords Electrochemical capacitors · Cobalt hydroxide · Electrodeposition · Porous structure

Introduction

Over the past decades, electrochemical capacitors (ECs) have attracted great attention because of their higher power density and longer cycle life than conventional secondary batteries [1]. They have been considered for all kinds of power source applications such as auxiliary power sources for hybrid electric vehicles, short-term power sources for mobile electronic devices, etc. [2–5]. According to their different mechanisms of energy storage, the ECs can be divided into electric double-layer capacitors and redox pseudocapacitors. Presently, most work on EC utilizing has been focused on electrode materials because the performances of the ECs are highly dependent upon the nature of the electrode materials, such as compositions, structures, and surface areas, etc. Therefore, the study of electrode materials has raised more concern in recent years.

Generally, the electrode materials of ECs can be divided into the following types: porous carbon [6, 7], transition-metal oxides [2, 8], and conducting polymers [9, 10]. Porous carbon materials are known to have high surface areas (up to ~2,500 m^2 g^{-1}), but lower specific capacitances (up to ~280 F g^{-1}) than metal oxides in aqueous electrolytes [11]. Conducting polymer materials are considered to have relatively lower specific capacitances. Besides, the electrochemical stability is also another issue for their usage in some redox process [12, 13]. Transition-metal oxides and hydroxide materials have been considered as the most promising materials for electrochemical capacitors [14–17]. As a representative of transition-metal oxides, RuO_2 generated very high specific capacitances [18–20], but the high cost makes it impossible to be commercialized in most applications. Therefore, other lower-cost materials such as NiO [21, 22], $Co(OH)_2$ [2, 23], $Ni(OH)_2$ [24, 25], MnO_2 [26, 27], and CoO_x [28] have attracted considerable attention. Among these metal oxides and hydroxides, cobalt hydroxide is becoming a promising electrode material due to its layered structure with large interlayer spacing [29, 30], well-defined electrochemical redox activity, and the possibility of the enhanced performance through different preparative methods [31].

L.-B. Kong (✉) · M.-C. Liu · J.-W. Lang · M. Liu
State Key Laboratory of Gansu Advanced Non-ferrous Metal Materials, Lanzhou University of Technology, Lanzhou 730050, People's Republic of China
e-mail: konglb@lut.cn

L.-B. Kong · Y.-C. Luo · L. Kang
School of Materials Science and Engineering, Lanzhou University of Technology, Lanzhou 730050, People's Republic of China

At present, there are several techniques to prepare cobalt hydroxide electrode materials, such as sol–gel method, chemical precipitation method, electrodeposition method, etc. Among these synthetic methods, electrodeposition method has several advantages. Firstly, active materials can be directly deposited on substrate without adding any polymer binder and conducting agent, the purity and conductivity of the active materials will not be affected by these additives. Secondly, active materials can be directly deposited on substrate rather than pressed at high pressure, thus, the microstructure of active materials will be preserved completely. Thirdly, weight and thickness of the active materials on substrate can be controlled simply by controlling the deposition conditions. Therefore, electrodeposition is an excellent method to prepare cobalt hydroxide electrode materials.

Recently, cobalt hydroxide films have been prepared by varied electrodeposition methods. Gupta and co-workers directly electrodeposited α-$Co(OH)_2$ film on stainless steel electrode [11]. In their report, nanolayered α-$Co(OH)_2$ sheets were electrodeposited on stainless steel electrode from 0.1 M cobalt nitrate electrolyte without adding any surfactant, but only 860 F g^{-1} of the specific capacitance was obtained because of the limited specific surface area of stainless steel electrode. A much higher specific capacitance of 2,646 F g^{-1} was achieved in Zhou's report [1], mesoporous α-$Co(OH)_2$ film was electrodeposited on nickel foam from cobalt nitrate dissolved in the aqueous domains of the hexagonal lyotropic liquid crystalline phase of Brij 56. However, this method was much complicated, and the high cost of the materials was another challenge to be commercialized in most applications.

In this study, porous α-$Co(OH)_2$ film with high specific capacitance has been successfully electrodeposited on nickel foam from 0.1 M $Co(NO_3)_2{\cdot}6H_2O$ solution without adding any surfactant. The microstructure and surface morphology of porous α-$Co(OH)_2$ film were characterized using X-ray diffraction (XRD) and scanning electron microscopy (SEM). The electrochemical properties of the film were investigated by means of cyclic voltammetry (CV), galvanostatic charge-discharge tests, and AC impendance spectroscopy in 1 M KOH aqueous solution electrolyte. What's more, effects of different deposition conditions such as deposition potential, deposition time, and different substrates on specific capacitance of α-$Co(OH)_2$ films were analyzed in detail.

Experimental

All the chemical reagents used in this experiment were analytical grade and used as received without further purification. $Co(NO_3)_2{\cdot}6H_2O$ and KOH were all purchased from Sinopharm Chemical Reagent Co. Ltd. Nickel foam was purchased from ChangSha Lyrun New Material Co. Ltd. The surface area of nickel foam for deposition was 1 cm^2 (1×1 cm). The nickel foam was washed in acetone with ultrasonic for 30 min at first, then washed with double-distilled water for several times, and dried in an oven at 60 °C.

The electrodeposition was performed in a standard three-electrode glass cell, a 1-cm^2 platinum plate was used as the counter electrode, and a saturated calomel electrode (SCE) was used as the reference electrode. Cobalt hydroxide films were directly deposited from 0.1 M $Co(NO_3)_2{\cdot}6H_2O$ solution at room temperature using a CHI660C electrochemical workstation (Chenhua, Shanghai). The deposition potential was −1.0 V vs.SCE. The electrodeposition process of the $Co(OH)_2$ film can be expressed as follows: [32]

$$NO_3^- + 7H_2O + 8e^- \rightarrow NH_4^+ + 10OH^- \quad (1)$$

$$Co^{2+} + 2OH^- \rightarrow Co(OH)_2 \quad (2)$$

After deposition process, cobalt hydroxide film on the nickel foam was washed with double-distilled water and dried in an oven at 40 °C for 12 h. In order to calculating the specific capacitance, the mass of active material is estimated by Faraday's law on the assumption that Faraday current efficiency for deposition is 100%. The weight of the deposite (m) can be calculated according to following equation:

$$m = \frac{5QM}{8N_A e} \quad (3)$$

where Q is the deposition charge, M is the relative molecular mass of $Co(OH)_2$, N_A is the Avogadro number, and e is the electronic charge.

XRD data were collected using a Rigaku D/MAX 2400 diffractometer (Japan) with Cu Kα radiation (λ=1.5418 Å) operating at 40 kV and 60 mA. The surface morphology of the $Co(OH)_2$ film was examined by SEM using a JEOL JSM-6700F (Japan). Electrochemical measurements were carried out in a three-electrode electrochemical cell; the working electrode was the prepared $Co(OH)_2$ electrode, a platinum plate, and an SCE were used as the counter electrode and reference electrode. Cyclic voltammetric, chronopotentiometric, and AC impendance measurements were performed on CHI660C electrochemical workstation (Chenhua, Shanghai).

Results and discussion

Structure and surface morphology characterization

Structural analysis of porous α-$Co(OH)_2$ film was carried out by X-ray diffraction technique, and the XRD patterns are

showed in Fig. 1. It can be seen that XRD pattern exhibits four major peaks. The first two peaks can be indexed as (001) and (002); they are related to d-spacings that are multiples of each other due to multiple reflections from the basal plane. However, the third and fourth peaks may belong to a group of different planes due to their different shapes from the first two peaks for their asymmetry between the high-angle side and the low-angle side; they can be indexed as (100) and (110). The XRD pattern of porous α-$Co(OH)_2$ film corresponds to the α-$Co(OH)_2$ [11, 33]. But, a case in point is that the (00*l*) reflections in Fig. 1 were not as strong as others prepared α-$Co(OH)_2$ [34, 35]. This may be due to the nano-size of the α-$Co(OH)_2$ sheets along the basal planes which results in a loss of intensity of the (00*l*).

The surface morphology of porous α-$Co(OH)_2$ film was illustrated by SEM. It can be seen from Fig. 2 that the film has sponge-like structure in low-magnification images, but the high-magnification images show that its network microstructure is consisting of many interlaced $Co(OH)_2$ leaves. These leaves grew perpendicular to the surface of nickel foam and left many pores. Such pore structure is much essential to the $Co(OH)_2$ film served as the electrode materials. On the one hand, these pores can provide passageway for ionic conduction and electrolyte diffusion in the film bulk. On the other hand, these porous structure provide higher specific surface area of the film, thus increase its specific capacitance.

Electrochemical measurements

Electrochemical capacitor properties of the prepared porous α-$Co(OH)_2$ film were elucidated by cyclic voltammetric, chronopotentiometric, and AC impendance measurements in 1 M KOH aqueous solution. Figure 3 shows the CV curves of porous α-$Co(OH)_2$ film deposited on Ni foam. For $Co(OH)_2$ electrode materials, it is well-accepted that the surface faradaic reaction at low potential can be expressed as follows:

$$Co(OH)_2 + OH^- \underset{\text{Discharge}}{\overset{\text{Charge}}{\rightleftharpoons}} CoOOH + H_2O + e^- \quad (4)$$

While the faradaic reaction at higher potential can be expressed as:

$$CoOOH + OH^- \underset{\text{Discharge}}{\overset{\text{Charge}}{\rightleftharpoons}} CoO_2 + H_2O + e^- \quad (5)$$

It can be seen from Fig. 3 that each CV curve consists of two pairs of visible redox peaks. This indicates that the measured pseudocapacitance is mainly governed by redox mechanism rather than pure electric double-layer capacitance. The strong anodic peak at negative potential is due to the oxidation of $Co(OH)_2$ to CoOOH and the strong cathodic peak is for the reverse process. The weak anodic peak at positive potential is corresponding to the oxidation of CoOOH to CoO_2, and the weak cathodic peak is for the reverse process. Moreover, because of its porous structure, ionic conduction and electrolyte diffusion in the film bulk was greatly improved; the shape of the CV curves was not significantly influenced with the increasing of the scan rates.

Figure 4 shows the first discharge curves of electrodeposited porous α-$Co(OH)_2$ film within the potential range of −0.1 to 0.45 V. The specific capacitance can be calculated according to the following equation:

$$C_m = \frac{C}{m} = \frac{I \times \Delta t}{\Delta V \times m} \quad (6)$$

Where C_m (farad per gram) is the specific capacitance, I (ampere) is discharge current, Δt (seconds) is the discharging time, ΔV (volt) represents the potential drop during discharge process, and m (grams) is the mass of the active material within the electrode. The prepared electrode materials exhibited excellent capacitive behavior at different current densities; the specific capacitance values calculated from discharge curves are 1,473, 1,337, 1,229, 1,107, and 987 F g^{-1} for porous α-$Co(OH)_2$ film discharged at current densities of 2, 4, 8, 16, and 32 A g^{-1}. The decrement of the specific capacitance at higher current densities is due to the increment of voltage drop and the insufficient active material involved in the redox reaction under higher current densities. Besides, it is clear that the decrement of the specific capacitance was not apparent due to the improved electrolyte diffusion and ionic conduction through porous structure in the film bulk. The result is very important for the porous α-$Co(OH)_2$ film to provide higher power density.

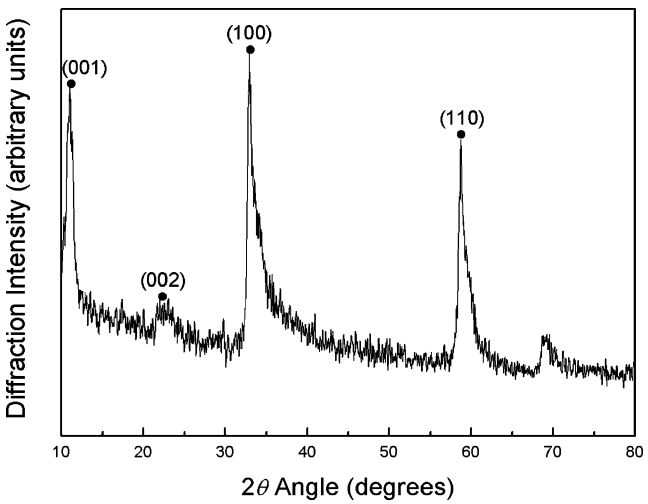

Fig. 1 X-ray diffraction patterns of electrodeposited porous α-$Co(OH)_2$ film

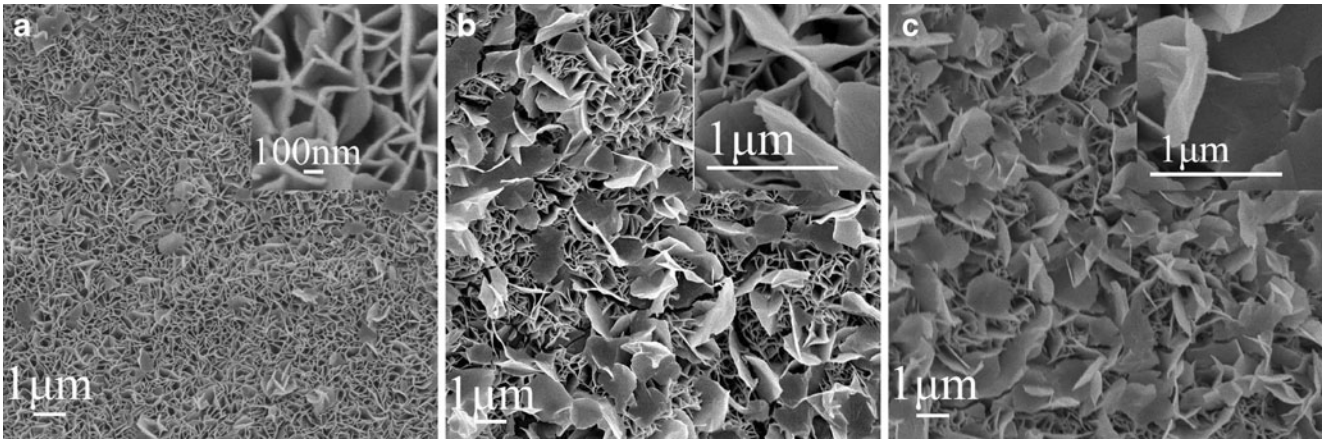

Fig. 2 SEM images of prepared porous α-$Co(OH)_2$ films deposited at different times **a** 100, **b** 140, and **c** 180 s

Another important aspect of a supercapacitor electrode is resistance. Figure 5 shows electrochemical impedance spectra in the form of Nyquist plots for prepared cobalt hydroxide electrode, where Z' and Z'' are the real and imaginary parts of the impedance. The plot in Fig. 5 is composed of a distorted semicircle like a plateau at high-frequency region and a line at low-frequency region. The plateau is due to the charge-transfer in faradaic reactions, and the straight line is related to the diffusion of ions in porous α-$Co(OH)_2$ film bulk. The observed electrode resistance was close to 1.3 Ω, which can be obtained from the intercept of the plots on the real axis. The relatively high electrode resistance is due to the poor electrical conductivity of cobalt hydroxide materials. The small diameter of distorted semicircle means low charge-transfer resistance because of improved ionic conduction and electrolyte diffusion through porous structure in the film bulk.

In order to demonstrate the electrochemical stability of porous α-$Co(OH)_2$ electrode materials, the charge–discharge cycling was carried out in 1 M KOH aqueous solution at the current density of 6 A g^{-1}. As shown in Fig. 6, the specific capacitance of the electrode decreases with the growth of the cycle number. After continuous 1,000 cycles, the capacitance value remains 88% of that of the early cycle. This means that electrodeposited porous α-Co$(OH)_2$ film has excellent electrochemical stability as an electrode material for electrochemical capacitors.

The effects of electrodeposition conditions on specific capacitance of porous α-$Co(OH)_2$ film

Electrodeposition conditions such as deposition time, deposition potential, different substrates, and concentration of Co$(NO_3)_2 \cdot 6H_2O$ solution were analyzed in detail to study their effects on specific capacitance and microstructure of the prepared porous α-$Co(OH)_2$ film.

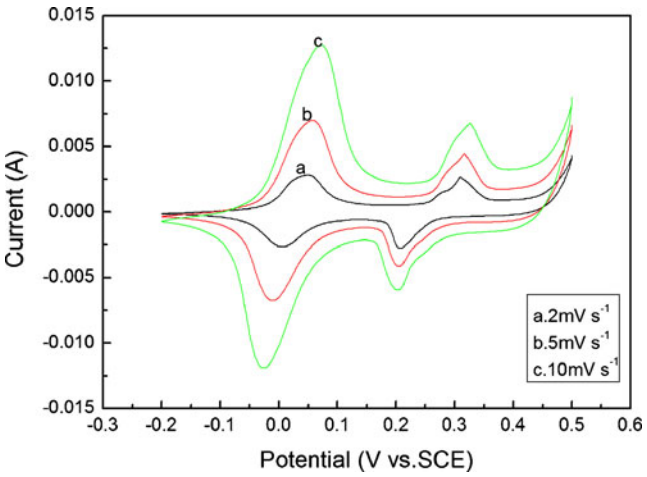

Fig. 3 CV curves of electrodeposited porous α-$Co(OH)_2$ film

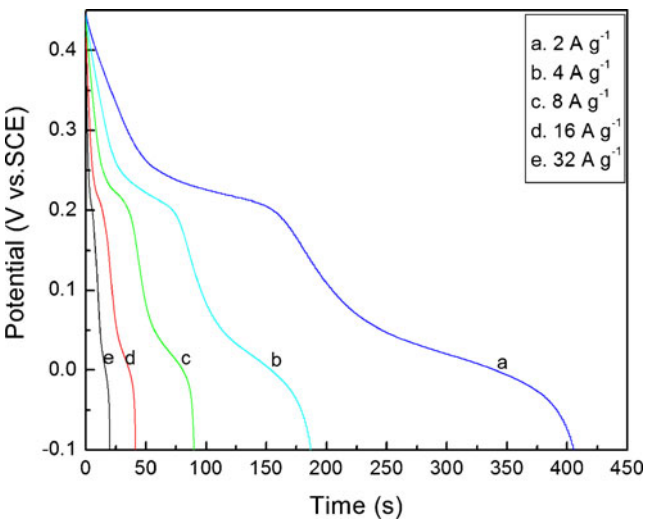

Fig. 4 First discharge curves of electrodeposited porous α-$Co(OH)_2$ film

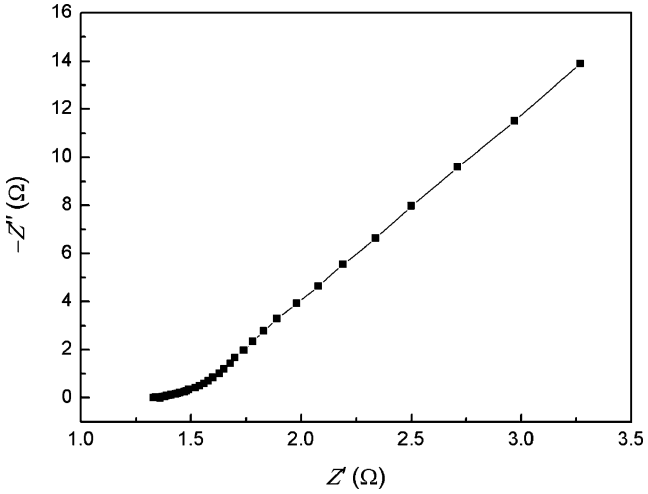

Fig. 5 Nyquist plots for the prepared cobalt hydroxide electrode

Effect of the deposition time on porous α-Co(OH)₂ films In order to investigate the effect of the deposition time on the surface morphology of deposited porous α-Co $(OH)_2$ film, SEM images of α-$Co(OH)_2$ films deposited at −1.0 V with different deposition times of 100, 140, and 180 s are displayed in Fig. 2a–c. It is evident that the surface morphology and microstructure of porous α-Co $(OH)_2$ films were significantly different. Comparing these low-magnification images, it is clear that a interlaced network porous microstructure was obtained at the deposition times of 100 s, but new $Co(OH)_2$ leaves began to grow along the surface of the film when the deposition time increased and much of pores were covered by these new Co $(OH)_2$ leaves. This suggest that at the beginning of the deposition process, $Co(OH)_2$ film grew perpendicularly to the surface of nickel foam, formed interlaced nanosheets structure and left lots of disordered pores. When the deposition time increased, it can be seen from the Fig. 2b, c that the former step was stopped, then the new $Co(OH)_2$ leaves began to grow along the surface of $Co(OH)_2$ film, and some of the pores were covered by the new growing films. Comparing these high-magnification images, it is clear that $Co(OH)_2$ leaves become larger with the increment of the deposition time, and the longer the deposition time, the more covered pores can be obtained. This was not the desired result because, when more pores were covered, the ionic conduction became less effective. Thus, the efficiency of faradaic reactions in the film bulk was reduced, and the specific capacitance was decreased. Figure 7 shows discharge curves of the $Co(OH)_2$ film deposited under −1.0 V at different deposition time. It can be seen that the $Co(OH)_2$ film deposited for 100 s has the highest specific capacitance. The decrement of the specific capacitance with the increase of the deposition time is due to the more and more covered pores in film bulk. The lower specific capacitance at shorter deposition time is because the $Co(OH)_2$ film was too thin to form a stable and effective porous structure.

Effect of the deposition potential on specific capacitance of porous α-Co(OH)₂ films The deposition potential is another important factor which will influence the specific capacitance of porous $Co(OH)_2$ film. First discharge curves of α-$Co(OH)_2$ film deposited at different potentials are shown in Fig. 8. It can be seen that film deposited at −1.0 V have the highest specific capacitance. On the one hand, when the potential become more positive, the speed of deposition will become slow, then the structure of the film will become compact, and the surface will become smooth. The pores in the film may be so small that these cannot serve as effective pores to transport electrolyte in faradaic

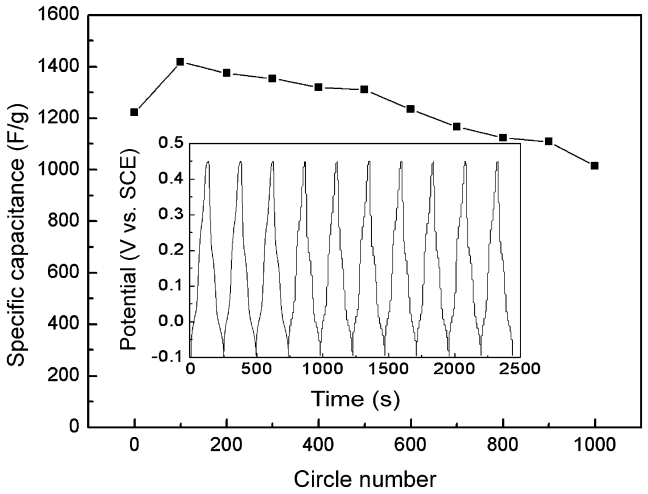

Fig. 6 Cycle life data of the prepared electrode at a discharge current density of 6 A g^{-1}

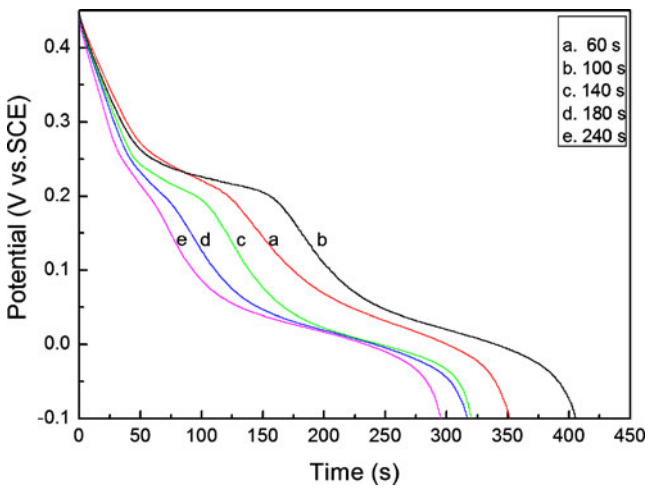

Fig. 7 First discharge curves of porous α-$Co(OH)_2$ films deposited at different deposition times

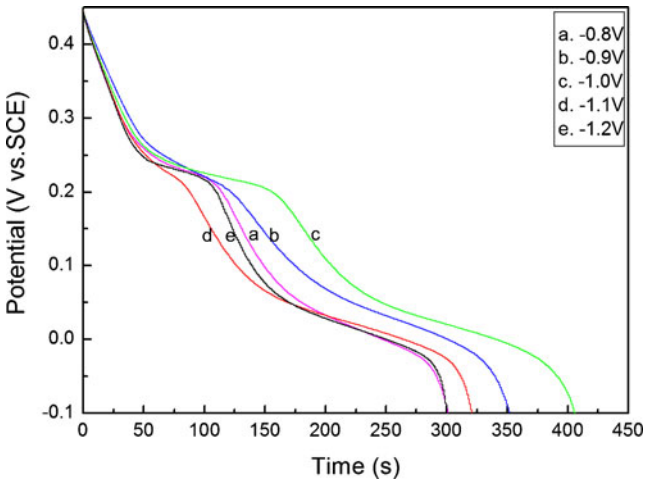

Fig. 8 First discharge curves of porous α-$Co(OH)_2$ films deposited at different potentials

reactions. This is the main reason that why the film deposited at higher potential have relatively low specific capacitance. On the other hand, when the potential become more negative, the speed of deposition will become too fast, that is to say, the speed of crystal growing will become too fast. The forming film will have rougher surface and larger pores, but low specific surface area. This is also a disadvantage to increase it is specific capacitance.

Effect of $Co(NO_3)_2{\cdot}6H_2O$ concentration on specific capacitance of porous α-$Co(OH)_2$ film Specific capacitance of porous α-$Co(OH)_2$ films deposited from different concentration of $Co(NO_3)_2{\cdot}6H_2O$ solutions are shown in Fig. 9. It is clear that the film with the highest specific capacitance was the one deposited from 0.1 M $Co(NO_3)_2{\cdot}6H_2O$ solution. When the concentration is too low, the speed of deposition will become slow, and then compact structure and smooth surface will be obtained. The pores in the film are too small to serve as channels for ionic conduction and electrolyte diffusion. Faradaic reaction in the film bulk will become less effective, and specific capacitance will be decreased. Conversely, when the concentration is too high, the speed of deposition will become too fast. The fast-growing crystals will forming larger pores, thus the surface area will be reduced. Such film also has lower capacitance.

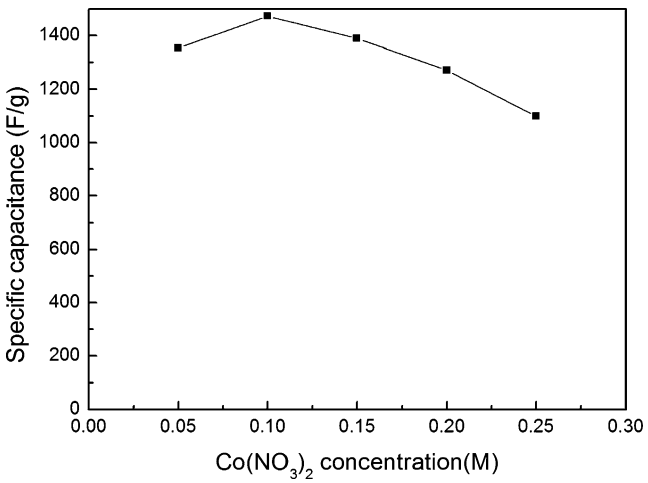

Fig. 9 Dependence of specific capacitance on the concentration of $Co(NO_3)_2{\cdot}6H_2O$ solution

Effect of different substrates on specific capacitance of porous α-$Co(OH)_2$ film Substrates have significant effects on specific capacitance of porous α-$Co(OH)_2$ films. Figure 10 shows discharge curves and CV curves of the film deposited on different substrates. It can be seen from Fig. 10a that the capacitance of porous α-$Co(OH)_2$ film on nickel foam is about two times that on nickel plate. Comparing the two CV curves in Fig. 10b, it is apparent that the CV curve of film deposited on nickel foam consists of two pairs of redox peaks while only one pair of peaks was found from the CV curve of the film deposited

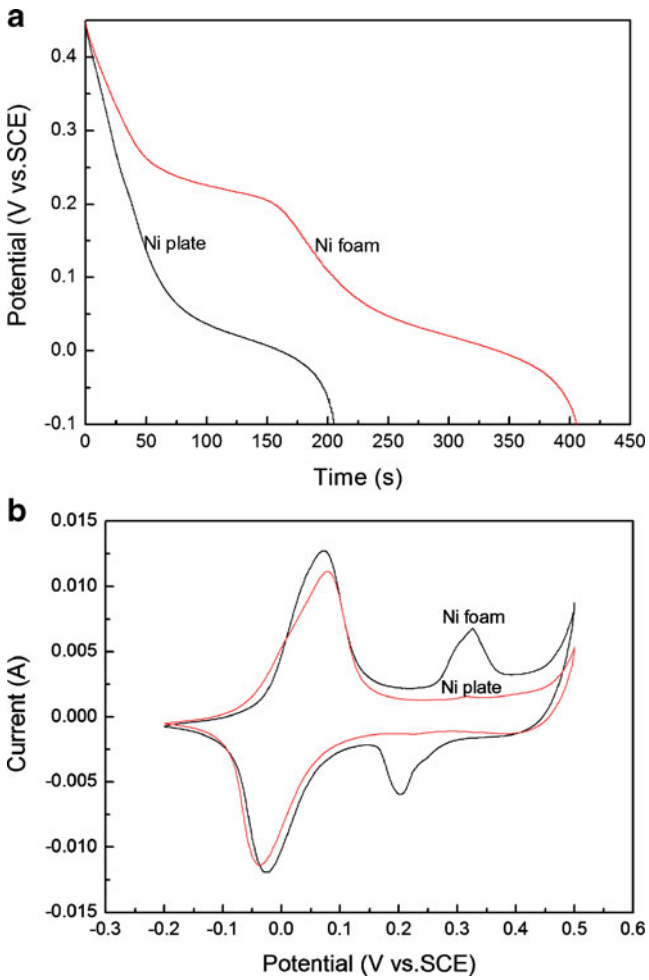

Fig. 10 **a** Discharge curves and **b** CV curves of porous α-$Co(OH)_2$ films deposited on different substrates

on nickel plate. This suggests that both faradaic reactions of (4) and (5) have occurred for $Co(OH)_2$ film deposited on nickel foam, but only reaction (4) has occurred for those on nickel plate. This is probably because the $Co(OH)_2$ film deposited on the three-dimensional structured nickel foam has a larger surface area and more reaction active sites due to the high distribution of the active materials. The $Co(OH)_2$ materials on nickel foam may undergo a much more sufficient and complete redox reaction.

Conclusion

In conclusion, we present a facile method to electrodeposite porous α-$Co(OH)_2$ films on nickel foam. It is the first time to directly electrodeposit porous α-$Co(OH)_2$ films on nickel foam using such a simple method without adding any surfactant. Structure study indicates that the prepared α-$Co(OH)_2$ film has interlaced network porous structure. Electrochemical measurements indicate that the porous $Co(OH)_2$ film has excellent supercapacitor behavior, with a maximum specific capacitance value of 1,473 F g^{-1}. Charge–discharge cycle illustrates that the prepared porous $Co(OH)_2$ film has excellent electrochemical stability. Besides, we found that electrodeposition time, deposition potential, and different substrates have significant effects on electrochemical capacitance of porous α-$Co(OH)_2$ films. We also found that film on nickel foam has much higher specific capacitance than film on nickel plate due to its larger surface area. In a word, the prepared porous α-$Co(OH)_2$ film is an excellent electrode material for supercapacitors.

Acknowledgements This work was supported by the National Natural Science Foundation of China (no. 50602020), the National Basic Research Program of China (no. 2007CB216408), and the Program for Outstanding Young Teachers in Lanzhou University of Technology (no. Q200803).

References

1. Zhou WJ, Zhao DD, Xu MW, Xu CL, Li HL (2008) Electrochim Acta 53:7210
2. Cao L, Xu F, Liang YY, Li HL (2004) Adv Mater 16:1853
3. Zhao DD, Zhou WJ, Li HL (2007) Chem Mater 19:3882
4. Yang GW, Xu CL, Li HL (2008) Chem Commun: 6537
5. Burke A (2000) J Power Sources 91:37
6. Wang DL, Li F, Liu M, Lu GQ, Cheng HM (2008) Angew Chem Int Ed 47:373
7. An KH, Kim WS (2001) Adv Funct Mater 11:387
8. Ke YF, Tsai DS, Huang YS (2005) J Mater Chem 15:2122
9. Fan LZ, Hu YS, Maier J, Adelhelm P, Smarsly B, Antonietti M (2007) Adv Funct Mater 17:3083
10. Chen WC, Wen TC, Teng H (2003) Electrochim Acta 48:641
11. Gupta V, Kusahara T, Toyama H, Supta S, Miura N (2007) Electrochem Commun 9:2315
12. Takasu Y, Murakami Y (2000) Electrochim Acta 45:4135
13. Hu CC, Tsou TW (2002) Electrochim Acta 47:3523
14. Sugimoto W, Iwata H, Yasunaga Y, Murakami Y, Takasu Y (2003) Angew Chem Int Ed 42:4092
15. Hu CC, Huang YH, Chang KH (2002) J Power Sources 108:117
16. Lee HY, Goodenough JB (1999) J Solid State Chem 144:220
17. Broughton JN, Brett MJ (2004) Electrochim Acta 50:4814
18. Srinivasan V, Weidner JW (2002) J Power Sources 108:15
19. Zheng JP, Cygan PJ, Jow TR (1995) J Electrochem Soc 142:2699
20. Park BO, Lokhande CD, Park HS (2004) J Power Sources 134:148
21. Liu KC, Anderson MA (1996) J Electrochem Soc 143:124
22. Nam KW, Kim KB (2002) J Electrochem Soc 149:A346
23. Jayashree RS, Kamath PV (1999) J Mater Chem 9:961
24. Cao L, Kong LB, Liang YY, Li HL (2004) Chem Commun 14:1646
25. Zhao DD, Bao SJ, Zhou WJ, Li HL (2007) Electrochem Commun 9:869
26. Xue T, Xu CL, Zhao DD, Li XH, Li HL (2007) J Power Sources 164:953
27. Prasad KR, Miura N (2004) J Power Sources 135:354
28. Lin C, Ritter JA, Popov BN (1998) J Electrochem Soc 145:4097
29. Ramesh TN, Rajamathi M, Kamath PV (2003) Solid State Sci 5:751
30. McNally EA, Zhitomirsky I, Wilkinson DS (2005) Mat Chem Phys 91:391
31. Ganesh V, Lakshminarayanan V, Pitchumanib S (2005) Electrochem Solid-State Lett 8:A308
32. Wang XF, You Z, Ruan DB (2006) Chin J Chem 24:1126
33. Djurfors B, Broughton JN, Brett MJ, Ivey DG (2005) Acta Mater 53:957
34. Zhang ML, Liu ZX (2002) Chin J Inorg Chem 5:513
35. Yuan C, Zhang X, Geo B, Li J (2007) Mat Chem Phys 101:148